Exploiting Bistability for High Force Density Reflexive Gripping

Rianna Jitosho, Kevin Choi, Adam Foris, and Anirban Mazumdar, Member, IEEE

Abstract— Robotic grasping can enable mobile vehicles to physically interact with the environment for delivery, repositioning, or landing. However, the requirements for grippers on mobile vehicles differ substantially from those used for conventional manipulation. Specifically, grippers for dynamic mobile robots should be capable of rapid activation, high force density, low power consumption, and minimal computation. In this work, we present a biologically-inspired robotic gripper designed specifically for mobile platforms. This design exploits a bistable shell to achieve "reflexive" activation based on contact with the environment. The mechanism can close its grasp within 0.12s without any sensing or control. Electrical input power is not required for grasping or holding load. The reflexive gripper utilizes a novel pneumatic design to open its grasp with low power, and the gripper can carry slung loads up to 28 times its weight. This new mechanism, including the kinematics, static behavior, control structure, and fabrication, is described in detail. A proof of concept prototype is designed, built, and tested. Experimental results are used to characterize performance and demonstrate the potential of these methods.

I. INTRODUCTION

Designs in the field of mobile robotics are largely constrained by the vehicle's limited battery life and payload capacity. Consequently, end effectors for these applications must be light, strong, and energy efficient. In addition, mobile systems are often difficult to precisely position due to their nonlinear dynamics, relatively low bandwidth, and limited onboard sensing. As a result, electrically driven servo type grippers are not always the best approach for mobile robotic systems.

Lightweight, adaptive grippers have been explored as alternatives to traditional end-effectors. Some solutions achieve adaptability by using compliant materials or underactuated mechanisms [1]-[4]. Other solutions implement claw-like mechanisms that can be purely rigid or may combine rigid and flexural members for gripping uneven surfaces [5]-[7]. While such designs can be lightweight and adaptable, they generally require sensing and control which increase complexity, weight, and power consumption.

In this study, we draw inspiration from biology and examine sensor-free reflexive grasping. Biological reflexes are stereotyped behaviors that are not centrally regulated by the brain [8]. This reflexive behavior can enable rapid response, computationally simple control, and reduced sensing requirements. The benefits of reflexive behaviors

Research supported by the National Science Foundation Summer Research for Undergraduates Program (NSF SURE).

R. Jitosho is with the Department of Mechanical Engineering at MIT, Cambridge, MA 02139 (e-mail: rjitosho@mit.edu).

K. Choi, A. Foris, and A. Mazumdar are with the Woodruff School of Mechanical Engineering at Georgia Tech, Atlanta, GA 30313 (email: anirban.mazumdar@gatech.edu).

have been demonstrated in biology. For example, the closing of the human hand can be easily coordinated and results from reflexive interactions between muscles in the hand instead of full regulation by the brain [8]. In a similar vein, we propose a simple approach that does not rely on regulation by a processing unit. Specifically, our engineered reflexive gripper uses no sensing or controls, and instead exploits flexible, bistable mechanics. The result is a bistable mechanism with two stable configurations. A small energy input from contact with the environment can cause the mechanism to transition from one configuration to another. The reflexive closing behavior is illustrated in Fig. 1.



Fig. 1. A visual illustration of our bi-stable gripper design closing when activated with by a mechanical collision with a tube.

Reflexive grippers utilize their mechanical design to activate a grasp rather than relying on sensing and electronic feedback. This type of "passive gripping" approach has the potential to reduce weight and complexity, and is therefore ideal for mobile robots such as unmanned aerial vehicles. Dry adhesive designs have already demonstrated impressive performance by utilizing landing forces to engage gecko-inspired pads [9], [10]. Other innovative passive mechanisms use the drone weight to actuate grasping [11], [12]. Recent works use the Fin Ray Effect to produce a gripping effect that does not require power to maintain a closed grasp [13].

Our work differs from these previous works through its use of a pre-stressed bistable structure. Bistable structures have two stable equilibrium states. This means that they can remain in each of these states without any energy input or control. Energy input is only needed to transition between the equilibrium states. Such mechanisms have been exploited in a variety of applications, from beam buckling to membrane deformation [14]-[18]. The method of actuation may utilize mechanics, electrostatics, magnetism, or thermodynamics [19]-[22]. Similarly, the use of bistable structures has previously been studied for achieving dramatic shape change and large motions [23]-[28].

Pre-stressed bistable behavior can result from deformations in the forming process that produce residual stresses [29]-[32]. The use of pre-stressed bistable mechanisms has been explored in small-scale applications [33]-[35] as well as aerospace release mechanisms [36]. In our work, we focus on rapid, lightweight, and repeatable gripping to hold a load in tension. This type of "prehensile"

gripping enables hanging from perches, brachiation, and the transportation of slung loads. This differs from prior work in bistable grippers such as the robot tongue presented by Cohen et al. [37], as we present a gripper with an interference structure allowing it to hold heavy loads with a prehensile grasp. Our work also provides detailed analysis and experimental characterization of gripper kinetics and holding force performance.

In this paper, we first outline our functional requirements for the overall reflexive gripping framework. We then describe the pre-stressed bistable metal shell and its behavior. This is followed by a discussion of our novel containment mechanism and the activation kinetics. These principles are incorporated into a fully functional prototype that uses a unique pneumatic system to open the grasp with minimal energy input and miniature components. We conclude by experimentally quantifying the performance.

II. FUNCTIONAL REQUIREMENTS

For a gripper to be suitable for dynamic mobile robotic applications, weight, energy consumption, and speed of activation are the most critical considerations. Based on these criteria, we outline the following functional requirements. These requirements are based on our desire to emulate biological performance as well as our own practical experience with mobile robotics.

- No sensing or control for grasp activation. We seek to reduce computing, sensing, and mass requirements by eliminating control during grasp activation.
- 2. *An activation time under 0.15 s*. This is comparable with biological reflexes [8].
- 3. *No energy input for holding a closed grasp.* This means that the duration of gripping does not affect robot performance and enables sustained gripping.
- 4. Hanging force density above 10:1. The endurance of mobile robots often depends on their weight. Thus, grippers must carry substantially large payloads as compared to the weight of the gripper itself.
- 5. Electrically resettable grasping. The ability to selectively open the gripper enables a broad range of applications including temporary perching, payload transport, and manipulation. Therefore, we seek a gripper design that can be opened via controlled electric energy input.
- 6. **Prehensile grasp capacity for a range of sizes**. We seek the ability to grasp a range of geometries. While load transport can utilize a known geometry, perching in unstructured environments may encounter a range of object sizes.

Our examination of the existing literature did not provide an overall approach that could meet all aforementioned functional requirements. Therefore, we chose to explore new approaches to robotic grasping. Specifically, we chose to focus on a novel approach that combines bistable prehensile grasping, high-friction surfaces, and pneumatic actuation. These systems can be activated with small amounts of mechanical energy input and can enable very rapid grasping. The use of high-friction surfaces enables large load bearing capacity. Pneumatic actuation enables dramatic shape change, lightweight components, and minimal power consumption. In the following sections, we describe our novel gripper in detail.

III. UTILIZING PRE-STRESSED BISTABLE BANDS

Pre-stressed bistable bands form the basis for our reflexive gripper design. Long strips of spring steel with a longitudinal axis, y, can be provided a positive initial curvature, κ_y , through plastic deformation. This plastic deformation can be achieved through heat treatment and subsequent plastic bending [29]. This is a stable state (grasp open). A second stable state (grasp closed) is when the band has a negative curvature about the transverse, x, axis. We call this curvature κ_y .

The band now possesses two stable states. In either state, the shell exhibits a curvature. The axes of curvature for each stable state are orthogonal to each other. A visualization of the two states as well as the naming convention is defined in Fig. 2. Since the open and closed configurations are both stable, they do not require any input power to remain in those states.

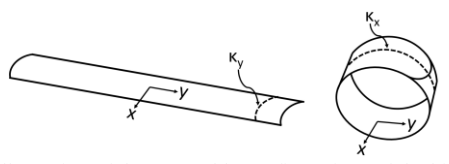


Fig. 2. An Illustration of the two stable configurations of the bistable metal band. On the left is the open state and the radius of curvature lies in the xz plane. On the right is the closed state and the radius of curvature lies in the yz plane.

A conceptual energy landscape for a pre-stressed steel band is shown in Fig. 3. The mechanical potential energy, U_M , is plotted against a displacement coordinate, X_{furl} , that represents the amount the strip is unfurled. Note that locations on the curve where the slope is zero represent equilibrium states where the net forces balance. The two equilibrium states (state 2 and state 5) for the pre-stressed steel strip are stable (positive $2^{\rm nd}$ derivative). This means that small displacements around the equilibrium states cause the system to return to equilibrium. This is ideal for a low-power gripper because external energy is not required to maintain the gripper configuration.

If sufficient external energy is added to the bistable band, it can transition between the equilibrium states. As Fig. 3 illustrates, a relatively small energy input can cause a transition from state 5 to state 2. This energy input can be used to activate a grasp closure. This enables a rapid,

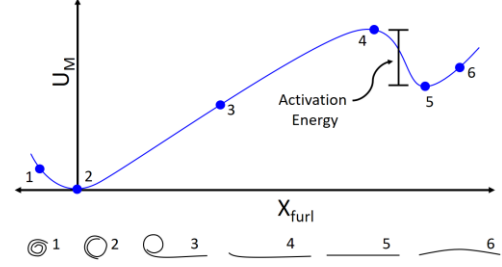


Fig. 3. A conceptual sketch of the general energy landscape of a prestressed steel strip.

reflexive gripper. We refer to this quantity as the "activation energy." We describe state 2 as a "closed grasp" and state 5 as an "open grasp."

The use of bistable mechanics to achieve grasp closure has several benefits. First, the grasp can be closed very quickly because it is not dependent on any actuation, sensing, or communication dynamics. In addition, the activation energy can be carefully quantified and used to inform the interaction of the gripper with the environment. activation energy can be quite low, thereby enabling grasp closure with minimal physical interaction. The gripper merely requires mechanical energy input to close. Finally, due to their prevalence in tools and wearable devices, a wide range of pre-stressed bistable bands made of spring steel is commercially available.

IV. BISTABLE GRIPPING MECHANISM

While a pre-stressed steel band enables rapid, simple, and energy efficient usage, careful mechanical design is required to maximize performance. Pre-stressed bistable bands have not been previously utilized for robotic prehensile-type grippers, and therefore require unique mechanisms to capture the band while still enabling it to open and close.

A custom containment mechanism was designed to hold the band and transmit forces while still enabling the band to close when activated. When the band closes, its configuration changes from flat to curved. Any containment mechanism must therefore allow this motion while restricting all other degrees of freedom. We achieve this by first constraining the band with four pieces that have protruding features designed to engage with notches in the steel band. These interfacing pieces determine the configuration of the In order to achieve a closed grasp, these band constraints must rotate and translate with the surface of the band. To accommodate this motion, band constraints are attached to axles that are in turn connected to geared links. This arrangement, shown in Fig. 4, enables the constraints to translate and rotate.

V. ACTIVATION KINETICS

A closed grasp is activated when energy is applied to the shell in the form of a downward displacement. This causes κ_y to go to zero and causes the curvature about the x-axis to increase in magnitude. This continues until there is large bending deformation about the x-axis and the transition to shell curvature κ_x . This rapidly propagates along the remainder of the shell, completing the activation process.

Recall that the activation energy, U_{Act} , is the amount of energy required to transition from the locally stable equilibrium (grasp open) to the global stable equilibrium (grasp closed). The activation energy can be treated as a force input with a corresponding displacement.

To estimate the activation energy, we utilize the strain energy model formulated by Kebadze [29]. The model considers a cylindrical shell element with an initial curvature k_{0c} in the x-direction (initially grasp closed configuration). Changes to the total strain energy can be parametrized with a single curvature value, κ_c , and the angle for the axis of curvature, θ . Based on this parametrization, the curvature

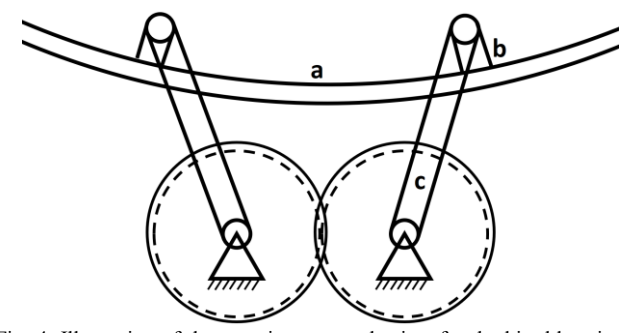


Fig. 4. Illustration of the containment mechanism for the bistable gripper. Shown are a) the steel band, b) band constraints capturing the steel band, c) geared links allowing translation and rotation of the plastic constraints.

changes in the local x, y coordinate system (Fig. 2) can then

be expressed through the following equations:
$$\Delta k_x = \frac{k_c}{2} (1 + \cos 2\theta) - k_{0c}$$

$$\Delta k_y = \frac{k_c}{2} (1 - \cos 2\theta)$$
(1)

$$\Delta k_y = \frac{\kappa_c}{2} (1 - \cos 2\theta) \tag{2}$$

$$\Delta k_{xy} = -\frac{k_c}{2}\sin 2\theta \tag{3}$$

Note that in the stable closed grasp (state 2), the associated strain energy is not zero, as internal stresses from the initial bending moment M_{oy} produce an energy approximately equal to U_I .

$$U_1 = \frac{M_{oy}^2 L}{2D(1 - v^2)} \tag{4}$$

where L is the band length, v is Poisson's ratio, and D is the band bending stiffness, which is expressed below. The quantities b and t are the band width and thickness, respectively.

$$D = \frac{Et^3b}{12(1-v^2)} \tag{5}$$

The bending moment M_{oy} performs work U_2 as the corresponding curvature Δk_v changes. Remaining curvature changes are captured in U_3 .

$$U_2 = M_{oy} \Delta k_y L \tag{6}$$

$$U_{3} = \frac{1}{2}DL[\Delta k_{x}^{2} + 2v\Delta k_{x}\Delta k_{y} + k_{y}^{2} + 2(1-v)\Delta k_{xy}^{2}]_{(7)}$$

The total strain energy is simply the sum:

$$U = U_1 + U_2 + U_3 \tag{8}$$

The original formulation in [29] assumed that all states were known based on the manufacturing process. In many cases (such as ours), an existing pre-stressed steel band may be utilized without knowledge of the overall manufacturing In this case, the material properties can be determined, and the curvature for the two stable states can be measured. However, the initial bending moment, M_{oy} , is unknown. Therefore, our proposed solution method is to solve iteratively by determining which value for M_{ov} results in a stable equilibrium at $\theta = 90^{\circ}$. Once this value is determined, then the activation energy can be determined by examining the strain energy landscape. This relatively simple methodology can be used to find order-of-magnitude estimates for the activation energy.

VI. GRASP OPENING MECHANISM

The design of a controlled electromechanical system that can unfurl the coiled steel band is non-trivial due to the complex continuous motions of the steel band. In addition, the need for lightweight and low power devices further reduces the types of applicable methods.

The high-deformation, continuous motions of bistable bands have many parallels to soft robotics. Distributed actuation techniques such as shape memory alloys, hydraulics, and pneumatics have all shown great promise in soft robotic technologies [37]-[41]. Shape memory actuators are one exciting method because they can deform to enable grasp closure and then return to their original shape when heated. However, the shape memory wires can interfere with the elastic behavior of the bistable band, thereby reducing grasp capacity. In addition, the heating of shape memory wires involves significant power consumption.

Therefore, we instead sought to explore fluid actuation. Pneumatic actuation is the most desirable for our application because the working fluid is lightweight, and a reservoir does not need to be carried on the mobile robot. For the unfurling mechanism, we drew inspiration from the Bourdon tube [42]-[44]. This device, historically used for pressure transducers, uses fluid pressure to straighten a curved pipe. In our case, we utilize a thin plastic channel as the tube, which curls when the gripper closes. The use of thin plastic results in minimal interference with the steel band behavior. When grasp opening is desired, pressurized air is pumped into the air channel, causing it to straighten.

While the mechanics of Bourdon tubes are nonlinear and complex, approximate results from existing works can be used to assess the pressure requirements for initiating opening of a fully closed grasp. Qualitative studies have shown that the grasp opens sequentially (one half unfurls, This means we can approximate the then the other). opening behavior by examining one side. We refer to the two halves of the band as "fingers."

The net moment applied by an internal pressure, P, can be described using the techniques outlined in [44]. This moment, M_u , acts about the Z-axis of the coordinate frame in Fig. 5. This moment is a function of the air channel geometric properties, and mainly the overall radius of curvature, \bar{R} . The tube cross section is approximated as an ellipse with semi major and minor axes, a, and b.

$$M_u = PaRD(1 - \cos\beta)k \tag{9}$$

$$D = a\left[\frac{4}{3}\left[\frac{K - E}{k^2} + (2E - K)\right] + \pi \frac{b}{a}\right]$$
 (10)

The variable k is used to parameterize the elliptical geometry.

$$k^2 = 1 - \frac{b^2}{a^2} \tag{11}$$

 $k^2 = 1 - \frac{b^2}{a^2}$ (11) The variables *K* and *E* are elliptical integrals of the first and second kind respectively. The moment imposed by the internal pressure, M_u , is resisted by the stiffness of the air channel and the internal moments of the steel band. Since our design is based on custom fabricated, thin plastic tubing, we neglect the stiffness of the air channel. The computed value for M_u is for the conditions near the initiation of grasp opening. This result can still provide insights into the

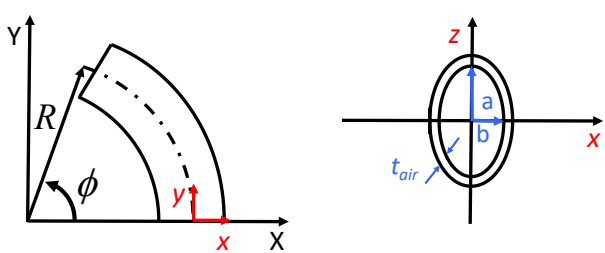


Fig. 5. A visual illustration of the pressurized unfurling approach based on Bourdon tube behavior.

relative pressure requirements for a given initial configuration. The value for M_u can be compared with the initial bending moment in the bistable band in order to determine how much pneumatic pressure is needed to start opening the grasp.

VII. PHYSICAL PROTOTYPE

A commercially available pre-stressed spring steel bistable shell was acquired by disassembling a "snap-band" type bracelet. This band has dimensions of 230 x 25 x 0.16 mm (length x width x thickness). The radii of curvature are $\kappa_{v} = 35.7 \text{mm}^{-1}$, and $\kappa_{x} = -13.1 \text{mm}^{-1}$.

The gripper can accommodate tubes or beams with diameters 25 ± 10mm. The containment mechanism was assembled from several custom-made components. Laser-cut geared links were attached to the 3D-printed base via steel axles. Small, 3D-printed pieces that constrain the band were attached to the rest of the containment mechanism via axles that passed through the geared links as well as the constraining pieces.

For controlled grasp opening, a lightweight, pneumatic solution was implemented. This pneumatic design enables small actuators, low power, and high flexibility. pneumatic mechanism does not interfere significantly with grasp closure and is well suited for mobile applications where weight and power are critical constraints.

An air channel was constructed with a heat sealer from 10⁻⁴ m thick ultra-high molecular weight polyethylene, and a third layer was attached to the channel to create a sheath for housing the bistable band. The channel is flat when empty and matches the curvature of the shell during activation without interfering with the gripper's ability to close. When the channel is inflated, the steel band unfurls. Once fully

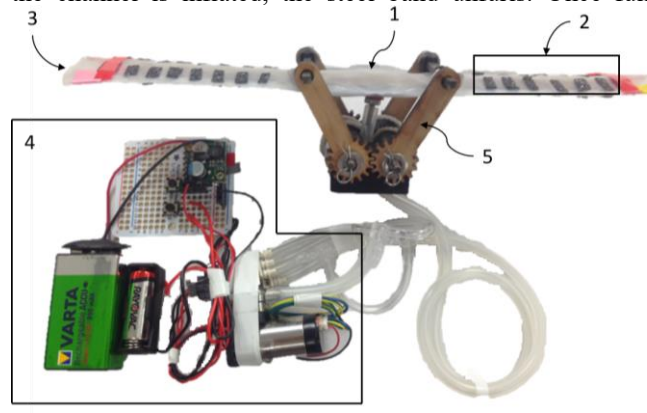


Fig. 6. Annotated photo of complete gripper prototype: 1. Bistable shell 2. Strips of high friction material 3. Pneumatic channel for reopening the gripper 4. Pneumatic actuation system for reopening 5. Containment mechanism.

unfurled, the band is in a stable equilibrium and does not require additional energy input to stay open.

The coefficient of friction between the two "fingers" of the gripper is very important for grasping loads smaller than the natural radius of curvature of the closed configuration. In order to maximize the holding force, an interference-type design was used. This design utilizes strips of grip-tape or sand paper. These provide both a high coefficient of friction as well as a form of mechanical interference that prevents unfurling under load. Bench level characterization provides an approximate friction coefficient of 2.5.

A TCS Brushless Micropump D250-BLZ-V was used to pressurize the air for the pneumatic system. This pump is capable of a maximum gauge pressure of 82.7kPa and a maximum flow rate of 0.017cm³/s. The pump is rated for 6V and consumes 0.6W when opening the grasp. A Pololu D24V25F6 buck converter was used to regulate the voltage so that standard batteries could be used. The pneumatic and electronic schematics for unfurling the bistable shell are illustrated in Fig. 7. Also shown in the diagrams are two 6V solenoid valves (S070C-VAG-32), each with three ports. These valves enable the use of a unidirectional pump to both inflate and deflate the gripper's air channel. This air pressure is projected to provide a moment of 1.6Nm at the instant of grasp opening. The total mass of all gripper mechanical components (band, containment mechanism, pump, valves, tubing) is 143g.

VIII. QUANTIFIED PERFORMANCE

A. Activation Kinetics

To quantify the activation energy, simulations based on Section V and physical experiments were performed. Numerical predictions for the energy landscape are shown in Fig. 8. For the given steel band, the activation energy was predicted to be 0.067J.

A 3-point bending test was also performed on the fully assembled prototype. The Mark-10 Mechanical Tester was utilized for these experiments. The experiment consisted of providing a downward displacement to the mechanism and measuring the force and displacement during this process. The experiment was performed until grasp closure was activated. The results are shown in Fig. 8. The integral of the experimental force-displacement curve provides the activation energy. This was calculated to be 0.026J. While

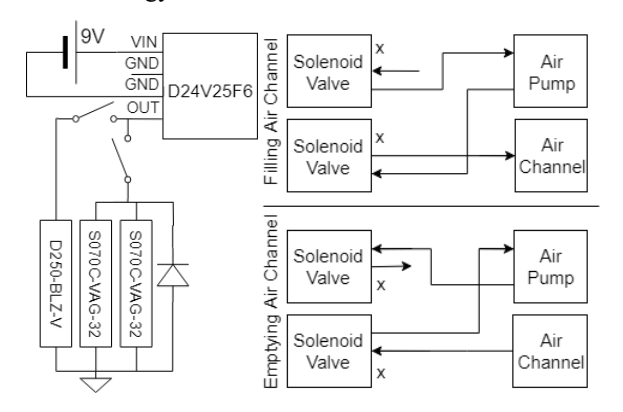


Fig. 7. Diagrams for the electronics (left) and pneumatics (right) which control the grasp opening process.

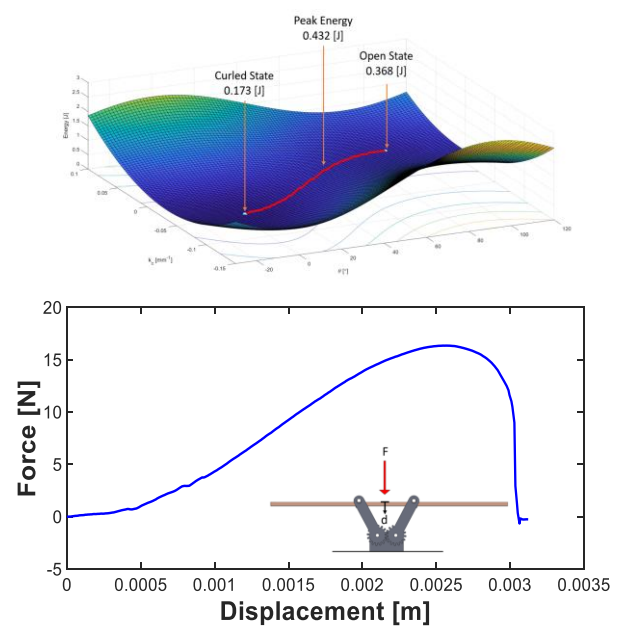


Fig. 8. Simulation for the energy landscape (above) and experimental results illustrating the behavior when activating a grasp closure (bottom).

this value is significantly lower than the analytical prediction, the error in J is small. The errors likely stem from uncertainties in the exact material properties of the steel band, the band forming process, discrepancies from the linear-elastic theory, and un-modeled behaviors stemming from the containment and grasp-opening mechanisms.

Both the experimental and theoretical results highlight the low activation energy of the prestressed steel band. The experimental value is equivalent to the energy from a 100g mass dropped from 27mm above the ground. This illustrates the small energy input required to activate a grasp closure. These experimental results also account for any potential interference from the air channel and the containment mechanism.

B. Hanging Force

To validate the gripper's ability to grasp a variety of objects, the load capacity was measured on steel pipes of varying diameters. As shown in the plot from Fig. 9, the holding force capacity increases with object diameter until a certain optimal diameter, after which the gripper's effectiveness begins to diminish. On a pipe too large, the gripper is not able to wrap around far enough to overlap its own fingers. The hanging force density of the reflexive gripper design ranges from 15 to 28.

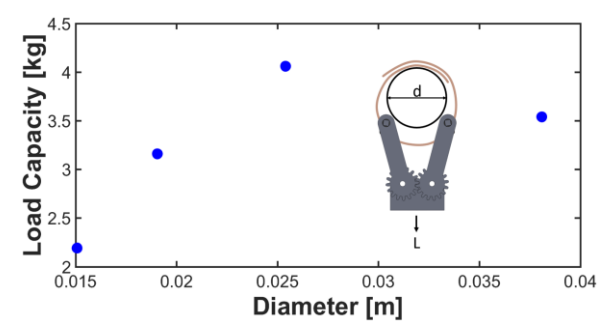


Fig. 9. Experimental data plotting load capacity for steel pipes of different diameters.

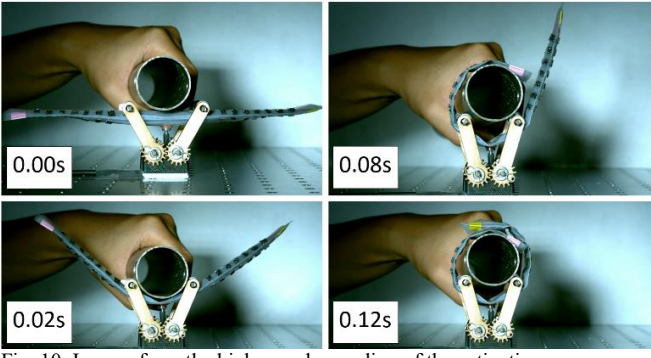


Fig. 10. Images from the high-speed recording of the activation process.

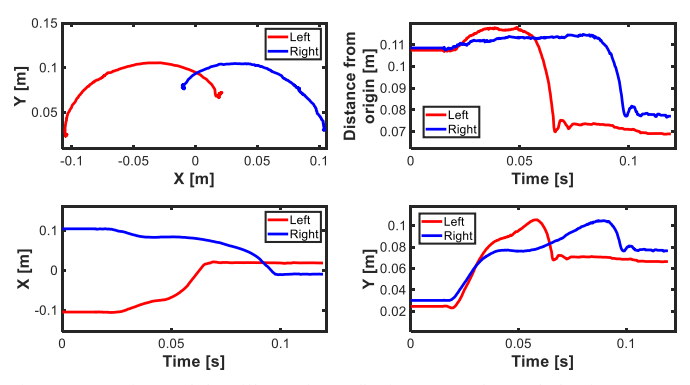


Fig. 11. Experimental data illustrating reflexive grasp closure behavior.

C. Reflexive Grasp Closure

High-speed photography was used to examine the reflexive grasp closure behavior. The mechanism was placed on an optical bench and activated by hand using a metal pipe moving at moderate speed. The gripper was labelled with colored tape in order to track its trajectory. Several images from the video are shown in Fig. 10. These images illustrate the speed at which the gripper deploys and fully closes when subject to a mechanical energy input.

Video processing software (Tracker) was used to measure the motion profiles of each end of the gripper. The trajectories are shown in Fig. 11. These results illustrate the symmetric nature of the tips and the speed at which deployment occurs. The grasp fully closes within 0.12s.

D. Pneumatic Grasp Opening

The pneumatic unfurling process was also examined using video data. The unfurling process is initiated by delivering 6V to the air pump. Unfurling video recordings and trajectories were collected using the same methodology as that of activation, and the results are shown in Fig. 12 and Fig. 13. The gripper unfurls in a controlled manner starting with the tip of the outside finger. The first finger unfurls nearly fully before the other finger starts unfurling. This simplifies analysis and reduces resistance to unfurling. The grasp unfurling is much slower (10s) than the grasp activation. Additionally, after the grasp is completely opened the inflated air channel must be excavated. This takes another 5s. If more rapid grasp opening is desired, a larger pump could be used. This would add weight and reduce grasp force density.

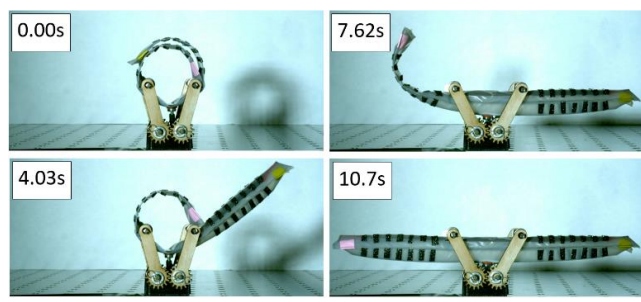


Fig. 12. Images from the high-speed recording of the unfurling process.

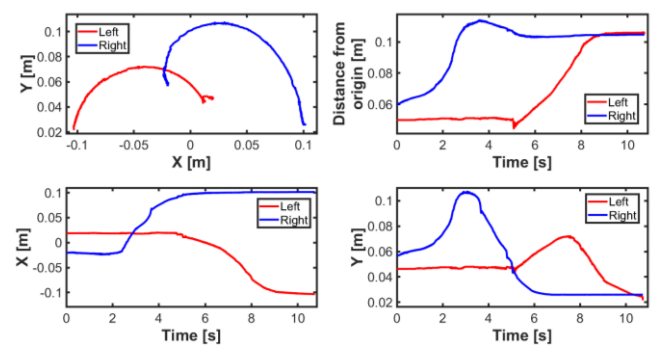


Fig. 13. Experimental data illustrating the gripper behavior during unfurling.

IX. CONCLUSION

In this work, we explored how bistable mechanisms can enable rapid and reflexive grasping. Reflexive bistable grasping has the potential to greatly simplify sensing and actuation. As a result, size, weight, and complexity can also be reduced. These attributes are particularly relevant to mobile robots such as unmanned aerial vehicles. We outlined a conceptual design, an innovative containment mechanism, and a unique pneumatic unfurling design.

A physical prototype was constructed and characterized experimentally. The experimental results demonstrate rapid grasp closure with speeds rivaling those of natural reflexes (0.12s). The activation energy needed to initiate grasp closure was shown to be very low (0.0264J), thereby enabling very sensitive performance. In addition, the physical prototype demonstrated high holding force densities (~15+) and unfurled with very little energy (12J). The bistable nature of the mechanism results in the property that no energy is required to hold the mechanism either open or closed. The primary limitation with this approach is the time needed to open the gripper (~15s). However, for many applications such as perching or carrying slung loads, this is not a big concern.

We believe that this new design will serve as an enabling technology for a broad range of mobile manipulation research. The ability to rapidly grasp an object through direct contact can enable new types of control and coordination architectures. These are especially relevant for mobile systems where precise position control can be very challenging.

ACKNOWLEDGMENT

The authors thank Zachary Goddard and Noe Monterrosa for their assistance with testing and troubleshooting.

REFERENCES

- M. E. Giannaccini, et al., "A variable compliance, soft gripper," Autonomous Robots, December 2013.
- [2] R. Deimel, O. Brock, "A novel type of compliant, underactuated robotic hand for dexterous grasping," Int. J. Rob. Res., August 2015.
- [3] V. Slesarenko, "Strategies to control performance of 3D-printed, cable-driven soft polymer actuators: from simple architectures to gripper prototype," Polymers, vol. 10, August 2018.
- [4] E. Brown, et al., "Univeral robotic gripper based on the jamming of granular material," Proc. Natl. Acad. Sci. U.S.A., vol. 107, November 2010.
- [5] J. Thomas, J. Polin, K. Sreenath, V. Kumar, "Avian-Inspired grasping for quadrotor micro UAVs," International Design Engineering Technical Conference and Computers and Information in Engineering Conference, August 2013.
- [6] G. Jung, J. Koh, K. Cho, "Underactuated adaptive gripper using flexural buckling," IEEE Trans. Rob., vol. 29, no. 6, December 2013.
- [7] M. Li, M. Su, R. Xie, Y. Zhang, H. Zhu, T. Zhang, Y. Guan, "Development of a bio-inspired soft gripper with claws," IEEE International Conference on Robotics and Biomimetics, December 2017.
- [8] E. R. Kandel, H. James, "Principles of neural science," 4th ed., McGraw-Hill, New York, 2000.
- [9] J. Thomas, et al., "Aggressive flight with quadrotors for perching on inclined surfaces," J. Mech. Rob., vol. 8, no.5, May 2016.
- [10] A. L. Desbiens, M. R. Cutkosky, "Landing and perching on vertical surfaces with microspines for small unmanned air vehicles," J. Intell. Rob. Syst., vol. 57, pp. 313–327, 2010.
- [11] M. Tieu, D. M. Michael, J. B. Pflueger, M. S. Sethi, K. N. Shimazu, T. M. Anthony, and C. L. Lee, "Demonstrations of bio-inspired perching landing gear for UAVs," Bioinspiration, Biomimetics, and Bioreplication, vol. 9797, 2016.
- [12] C. E. Doyle, et al., "Avian-inspired passive perching mechanism for robotic rotorcraft," Int. Conf. on Intell. Rob. Syst., 2011.
- [13] W. Crooks, S. Rozen-Levy, B. Trimmer, C. Rogers, W. Messner, "Passive gripper inspired by Manduca sexta and the Fin Ray Effect," Int. J. Adv. Rob. Syst., vol. 14 issue 4, July 2017.
- [14] B. D. Jensen, L. L. Howell, "Bistable configurations of compliant mechanisms modeled using four links and translational joints," J. Mech. Des., vol. 126, pp. 657-666, July 2004.
- [15] T. Ngo, H. Tran, T. Nguyen, T. Dao, D. Wang, "Design and kinetostatic modeling of a compliant gripper for grasp and autonomous release of objects," Advanced Robotics, 2018.
- [16] Q. Truong, N. Tran, D. Wang, "Design and characterization of a mouse trap based on bistable mechanism," Sens. Actuators, A, vol. 267, pp. 360-375, November 2017.
- [17] J. Tsay, L. Su, C. Sung, "Design of a linear micro-feeding system featuring bistable mechanisms," J. Micromech. Microeng., vol. 15, no. 1, October 2004.
- [18] D. S. Popescu, T. S. J. Lammerink, M. Elwenspoek, "Buckled membranes for microstructures," Proc. of the IEEE Microelectromech. Syst., pp. 188 – 192, February 1994.
- [19] B. Wang, K Fancey, "Shape-changing (bistable) composites based on viscoelastically generated prestress," 10th International Conference on Composite Science and Technology, September 2015.
- [20] K. J. Gabriel, O. Tabata, K. Shimaoka, S. Sugiyama, H. Fujita, "Surface-normal electrostatic/pneumatic actuator," Proc. of the IEEE An Investigation of Micro Structures, Sensors, Actuators, Machines and Robot, pp. 128 – 132, February 1992.
- [21] J. Zhao, R. Gao, Y. Yang, Y. Huang, P. Hu, "A bidirectional acceleration switch incorporating magnetic-fields-based tristable mechanism," IEEE/ASME Trans. Mechatron., vol. 18, no. 1, February 2013.
- [22] R. A. Lake, R. A. Coutu Jr., "Variable response of a thermally tuned MEMS pressure sensor," Sens. Actuators, A, vol. 246, pp. 156-162, August 2016.
- [23] M. Follador, A. T. Conn, J. Rossiter, "Bistable minimum energy structures (BiMES) for binary robotics," Smart Mater. Struct., vol. 24, June 2015.

- [24] M. Estrada, et al., "Free-flyer acquisition of spinning objects with gecko-inspired adhesives," IEEE Int. Conf. Rob. Autom., 2016.
- [25] A. Yamada, H. Mameda, H. Mochiyama, H. Fujimoto, "A compact jumping robot utilizing snap-through buckling with bend and twist," Proc. of the 2010 IEEE/RSJ Int. Conf. on Intell. Rob. Syst., 2010.
- [26] A. Yamada, Y. Sugimoto, H. Mochiyama, H. Fujimoto, "An impulsive force generator based on closed elastica with bending and distortion and its application to swimming tasks," IEEE Int. Conf. Rob. Autom., 2011.
- [27] S. Daynes, P. M. Weaver, "Review of shape morphing automobile structures: concepts and outlook," Proc. of the Institution of Mechanical Engineers Part D J. of Automobile Engineering, vol. 227, pp. 1603-1622, November 2013.
- [28] F. Nicassio, G. Scarselli, F. Pinto, F. Ciampa, O. Iervolino, M. Meo, "Low energy actuation technique of bistable composites for aircraft morphing," Aerosp. Sci. Technol., December 2017.
- [29] E. Kebadze, S.D. Guest, S. Pellegrino, "Bistable prestressed shell structures," Int. J. Solids Struct., vol. 41, June 2004.
- [30] Z. Chen, Q. Guo, C. Majidi, W. Chen, D. J. Srolovitz, M. P. Haataja, "Nonlinear geometric effects in mechanical bistable morphing structures," Phys. Rev. Lett., vol. 109, September 2012.
- [31] S. Yi, X. He, J. Lu, "Bistable metallic materials produced by nanocrystallization process," Mater. Des., vol. 141 pp 374-383, March 2018.
- [32] M. G. Walker, K. A. Seffen, "On the shape of bistable creased strips," Thin-Walled Structures, vol. 124, pp 538-545, March 2018.
- [33] T. Chen, J. Mueller, K. Shea, "Design and fabrication of a bistable unit actuator with multi-material additive manufacturing," Proc. of the 26th Annual International Solid Freeform Fabrication Symposium, August 2016.
- [34] Q. Xu, "Design of a large-stroke bistable mechanism for the application in constant-force micropositioning stage," J. Mech. Rob., vol. 9, November 2016.
- [35] Q. Han, K. Jin, G. Chen, X. Shao, "A novel fully compliant tensural-compresural bistable mechanism," Sens. Actuators, A, vol. 268, pp 72-82, December 2017.
- [36] S. A. Zirbel, K. A. Tolman, B. P. Trease, L. L. Howell, "Bistable mechanisms for space applications," PLoS ONE, vol. 11, December 2016.
- [37] C. Cohen, B. Hiott, A. Kapadia, I. Walker, "Robot tongues in space: continuum surfaces for robotic grasping and manipulation," Proc. SPIE Micro- and Nanotechnology Sensors, Systems, and Applications VIII, May 2016.
- [38] S. Seok, C. D. Onal, K. Cho, R. J. Wood, D. Rus, S. Kim, "Meshworm: a peristaltic soft robot with antagonistic nickel titanium coil actuators," IEEE/ASME Trans. Mechatron., vol. 18(5), October 2013.
- [39] J. Koh, K. Cho, "Omega-shaped inchworm-inspired crawling robot with large-index-and-pitch (LIP) SMA spring actuators," IEEE/ASME Trans. Mechatron., vol. 18, no. 2, April 2013.
- [40] L. Tiziani, A. Hart, T. Cahoon, F. Wu, H. H. Asada, F. L. Hammond, "Empirical characterization of modular variable stiffness inflatable streutures for supernumerary grasp-assist devices," Int. J. Rob. Res., vol. 36(13-14), pp. 1391-1413, 2017.
- [41] R. MacCurdy, R. Katzschmann, Y. Kim, D. Rus, "Printable hydraulics: a method for fabricating robots by 3D co-printing solids and liquids," IEEE Int. Conf. Rob. Autom., May 2016.
- [42] R. A. Clark, E. Reissner, "Deformation and stresses in bourdon tubes," J. App. Phys., vol 21, 1950.
- [43] N. N. Pak, R. J. Webster III, A. Menciassi, P. Dario, "Electrolytic silicone bourdon tube microactuator for reconfigurable surgical robots," IEEE Int. Conf. Rob. Autom., April 2007.
- [44] C. D. Conway, "Analytical analysis of tip travel in a bourdon tube," Master's Thesis, Naval Postgraduate School, 1995.